

Macroscopic electromagnetic response of metamaterials with toroidal resonances

V. Savinov,^{1,*} V. A. Fedotov,¹ and N. I. Zheludev^{1,2}

¹*Optoelectronics Research Centre & Centre for Photonic Metamaterials, University of Southampton, UK*

²*Centre for Disruptive Photonic Technologies, Nanyang Technological University, Singapore 637371, Singapore*

Toroidal dipole, first described by Ia. B. Zeldovich [Sov. Phys. JETP **33**, 1184 (1957)], is a distinct electromagnetic excitation that differs both from the electric and the magnetic dipoles. It has a number of intriguing properties: static toroidal nuclear dipole is responsible for parity violation in atomic spectra; interactions between static toroidal dipole and oscillating magnetic dipole are claimed to violate Newton's Third Law while non-stationary charge-current configurations involving toroidal multipoles have been predicted to produce vector potential in the absence of electromagnetic fields. Existence of the toroidal response in metamaterials was recently demonstrated and is now a growing field of research. However, no direct analytical link has yet been established between the transmission and reflection of macroscopic electromagnetic media and toroidal dipole excitations. To address this essential gap in electromagnetic theory we have developed an analytical approach linking microscopic and macroscopic electromagnetic response of a metamaterial and showed, using a case study, the key role of the toroidal dipole in shaping the electromagnetic properties of the metamaterial.

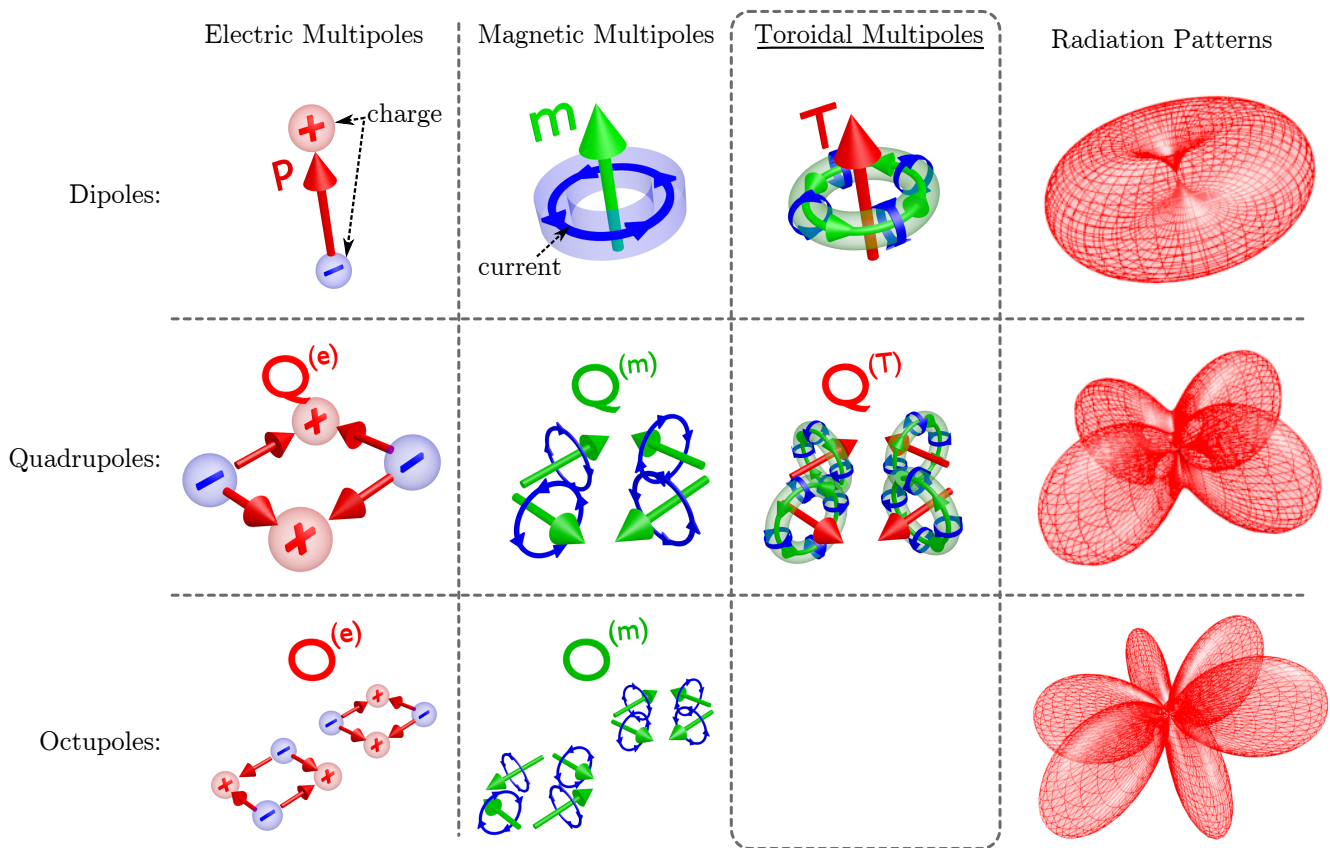


Figure 1: **The members from the three families of dynamic multipoles up to third order.** The three columns on the left show the charge-current distribution that give rise to the leading multipoles up to the third order. The included multipoles are the electric (\mathbf{p}), magnetic (\mathbf{m}) and toroidal (\mathbf{T}) dipoles, electric ($\mathbf{Q}^{(e)}$), magnetic ($\mathbf{Q}^{(m)}$) and toroidal ($\mathbf{Q}^{(T)}$) quadrupoles as well as the electric ($\mathbf{O}^{(e)}$) and magnetic ($\mathbf{O}^{(m)}$) octupoles. The toroidal dipole (\mathbf{T}), is created by the oscillating poloidal current - the current that flows along the meridians of a torus. The next member of the toroidal multipole family, the toroidal quadrupole ($\mathbf{Q}^{(T)}$), is created by the anti-aligned pairs of toroidal dipoles. The column on the right shows the patterns of radiation (i.e. intensity as a function of direction) emitted by the various harmonically oscillating multipoles (for quadrupoles, only the radiation associated with the off-diagonal component of the second-rank quadrupole moment tensor is shown, for octupoles only the radiation associated with the component of the third-rank octupole moment tensor with two repeated indices and the third distinct index is shown).

The discovery of the toroidal dipole can be traced back to Zel'dovich's original work¹ in 1957. It is the first member of the toroidal multipole family and is created by the currents flowing along the meridians of a torus (see Fig. 1). Since the discovery, the toroidal dipoles have been used to test the Standard Model², demonstrate strong optical activity³, and negative index of refraction⁴. The combination of dynamic magnetic and static toroidal dipoles has been predicted to violate Newton's Third Law⁵, whilst different opinions exist on whether the combination of dynamic electric and toroidal dipoles could lead to a non-radiating configuration, which emits no electromagnetic radiation despite being a source of propagating, non-trivial (un-removable by any gauge choice) vector potential⁶⁻⁹. Following the recent experimental demonstration of the toroidal dipole response in metamaterials¹⁰, the interest in this topic has been grow-

ing rapidly^{9,11-16} despite the lack of theory linking the microscopic toroidal electrodynamics to macroscopic observables such as transmission and reflection. In this paper we develop a fully analytical formalism to fill this gap.

The electromagnetic properties of media are generally described in terms of macroscopic material parameters (such as, for example, dielectric permittivity ϵ and magnetic permeability μ) that through constitutive relations establish a connection between the media's macroscopic response and microscopic charge-current excitations induced by the electromagnetic fields in media's constituents, i.e. atoms or molecules¹⁷. Such description is being also applied to the so-called metamaterials, man-made material composites with exotic electromagnetic properties achieved through structuring on the sub-wavelength scale¹⁸⁻²⁰. However, obtaining effective ma-

terial parameters for the metamaterials is not straightforward and often impossible due to their structural inhomogeneity and strong spatial dispersion^{21,22}.

Here we present a formalism that allows one to calculate the transmission and reflection of two-dimensional metamaterials (as well as the films of sub-wavelength thickness made from conventional materials) based directly on the multipolar decomposition of the microscopic charge-current excitations, thus avoiding the need for introducing the effective material parameters. Similar problem of calculating the scattered radiation from arrays of metallic resonators have been addressed in the past using Fast Multipole Method (FMM)^{23–27}, and periodic Green’s functions for the Helmholtz equation^{28–30}. What makes our approach different, is that it yields expressions sufficiently compact to be suitable not only for computer-aided calculations (like FMM), but also for the purely analytic evaluation. At the same time our approach accounts not only for the conventional multipoles but also for the elusive toroidal multipoles (see Fig. 1). By applying the derived formalism to a test case study metamaterial, we show that characterization of the electromagnetic response of a certain class of structures is greatly enhanced by taking the toroidal multipoles into account.

We will now proceed to deriving a general expression for the electromagnetic field scattered by a two-dimensional array of identical charge-current excitations that are represented by a finite series of dynamic multipoles. For the case of a passive materials (and metamaterials), these multipoles would be induced by normally incident plane wave. We assume that the multipole moments can either be extracted from the numerical simulation of the induced currents, or can be calculated from the anticipated dynamics of charge and current densities induced in the meta-molecules of a particular geometry by the incident radiation^{31–35}. In the interest of brevity only the key steps of the derivation will be demonstrated by finding the expression for the radiation from a two-dimensional sub-wavelength array of toroidal dipoles, before giving the full expression that includes all lower-order multipoles.

We start from the far-field distribution of the electric field radiated by a single oscillating toroidal dipole, which has been derived by Radescu & Vaman in³⁶ (also see Appendix):

$$\mathbf{E}(\mathbf{r}) = \frac{-i\mu_0 c^2 k^3}{3\sqrt{2\pi}} \cdot \frac{\exp(-ikr)}{r} \cdot \sum_{m=0,\pm 1} T_{1m} \left[\mathbf{Y}_{1,2,m} + \sqrt{2}\mathbf{Y}_{1,0,m} \right] \quad (1)$$

$$T_{1,\pm 1} = \frac{1}{\sqrt{2}} (\mp T_x + iT_y) \quad (2)$$

$$T_{1,0} = T_z \quad (3)$$

$$\mathbf{T} = \frac{1}{10c} \int d^3r \left[\mathbf{r}(\mathbf{r} \cdot \mathbf{J}) - 2r^2 \mathbf{J} \right] \quad (4)$$

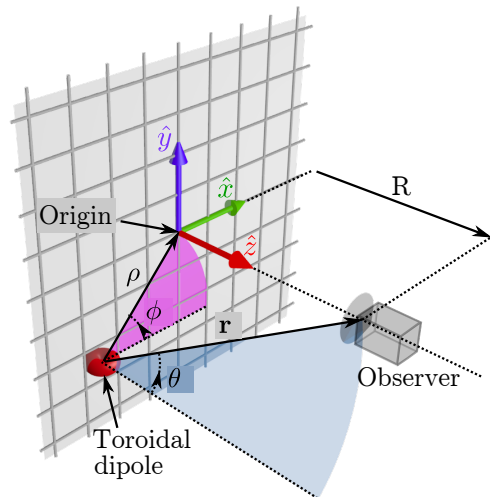


Figure 2: **Calculating scattering from a two-dimensional planar array of toroidal dipoles.** A single toroidal dipole is represented by its radiation pattern. The vectors connecting the dipole to the observer and to the origin of the array are \mathbf{r} and ρ , respectively. The observer is located at distance R from the array. The vector \mathbf{R} is perpendicular to the array plane. The position of the observer relative to the dipole in spherical polar coordinates is (r, θ, ϕ) .

Here μ_0 is the magnetic permeability of vacuum, c is the speed of light, \mathbf{r} is the vector connecting the location of the dipole with the observer and $\mathbf{Y}_{l,l',m}$ are the spherical vector harmonics that allow to represent any vector field on the surface of the unit sphere in the same way as spherical harmonics allow to represent any scalar field on the surface of the unit sphere^{36–38}. The (Cartesian) toroidal dipole is denoted by \mathbf{T} , whilst \mathbf{J} is the current density that gives rise to dipole. Unlike Vaman & Radescu³⁶, we are using the SI units and assume harmonic time-dependence specified by $\sim \exp(+i\omega t)$, where ω is the angular frequency and $k = 2\pi/\lambda = \omega/c$ is the wavenumber.

The total field radiated by an infinitely large planar array of toroidal dipoles (\mathbf{E}_s) is obtained by summing the contributions from all the dipoles at the position of the observer. As stated above, we assume that all the dipoles oscillate in phase (i.e. the multipole array is induced by the plane wave at normal incidence), and that the unit cell of the array is smaller than the wavelength. The latter assumption allows to replace the sum over the unit cells with an integral over the array area (Δ^2 denotes the area of the unit cell).

$$\mathbf{E}_s = \sum_{\mathbf{r}} \mathbf{E}(\mathbf{r}) \approx \frac{1}{\Delta^2} \int d^2r \mathbf{E}(\mathbf{r}) \quad (5)$$

We choose to work in the coordinate system where the array of dipoles lies in the xy -plane and the incident/scattered radiation propagates along the z -axis (see Fig. 2). Explicit evaluation of the relevant spherical vec-

tor harmonics produces³⁶:

$$\begin{aligned} & \mathbf{Y}_{1,2,\pm 1} + \sqrt{2}\mathbf{Y}_{1,0,\pm 1} = \\ & = \begin{pmatrix} \pm\sqrt{\frac{3}{10}}Y_{2,\pm 2} \mp \sqrt{\frac{1}{20}}Y_{2,0} \mp Y_{0,0} \\ -i\sqrt{\frac{3}{10}}Y_{2,\pm 2} - i\sqrt{\frac{1}{20}}Y_{2,0} - iY_{0,0} \\ -\sqrt{\frac{3}{10}}Y_{2,\pm 1} \end{pmatrix} \\ & \mathbf{Y}_{1,2,0} + \sqrt{2}\mathbf{Y}_{1,0,0} = \begin{pmatrix} \sqrt{\frac{3}{20}}Y_{2,1} - \sqrt{\frac{3}{20}}Y_{2,-1} \\ -i\sqrt{\frac{3}{20}}Y_{2,1} - i\sqrt{\frac{3}{20}}Y_{2,-1} \\ -\sqrt{\frac{2}{5}}Y_{2,0} + \sqrt{2}Y_{0,0} \end{pmatrix} \end{aligned}$$

The vectors are presented in the Cartesian basis with column entries indicating the x-, y- and z-components (from top to bottom respectively), $Y_{l,m}$ are the standard spherical harmonics³⁶. The basic integral that needs to be calculated in Eq. (5), after substitution of Eq. (1), is:

$$I_{l,m} = \int d^2r Y_{l,m} \exp(-ikr) / r \quad (6)$$

By assuming that the propagation of radiation occurs in space with losses, i.e. $\Im(k) < 0$, and by focusing on the far-field component of radiation, i.e. by assuming that the distance between the observer and the dipole array is significantly larger than the wavelength of radiation $R \gg \lambda$, one can show that (see Appendix):

$$I_{l,m} \cong \frac{\pi \delta_{m,0} (\hat{\mathbf{R}} \cdot \hat{\mathbf{z}})^l}{ik} \cdot \sqrt{\frac{2l+1}{\pi}} \cdot \exp(-ikR) \quad (7)$$

where $\hat{\mathbf{R}} = \mathbf{R}/R$ (see Fig. 2). Substitution of Eq. (1) into Eq. (5) and use of Eq. (7) allows to derive:

$$\mathbf{E}_s = \frac{\mu_0 c^2 k^2}{4\Delta^2} \cdot \sqrt{2} \cdot \begin{pmatrix} T_{1,1} - T_{1,-1} \\ i(T_{1,1} + T_{1,-1}) \\ 0 \end{pmatrix} \cdot \exp(-ikR)$$

Further simplification produces the final form:

$$\mathbf{E}_s = -\frac{\mu_0 c^2 k^2}{2\Delta^2} \mathbf{T}_{\parallel} \exp(-ikR) \quad (8)$$

where $\mathbf{T}_{\parallel} = \mathbf{T} - (\mathbf{T} \cdot \hat{\mathbf{R}})\hat{\mathbf{R}}$ denotes the projection of toroidal dipole into the plane of the array ($\mathbf{T}_{\parallel} = (T_x, T_y, 0)^T$ for the coordinate system as in Fig. 2). Repetition of the derivation given above for other multipoles results in:

$$\begin{aligned} \mathbf{E}_s = \frac{\mu_0 c^2}{2\Delta^2} \cdot & \left[-ik\mathbf{p}_{\parallel} + ik\hat{\mathbf{R}} \times \left(\mathbf{m}_{\parallel} - \frac{k^2}{10}\mathbf{m}_{\parallel}^{(1)} \right) - \right. \\ & \left. -k^2 \left(\mathbf{T}_{\parallel} + \frac{k^2}{10}\mathbf{T}_{\parallel}^{(1)} \right) + k^2 \left(\mathbf{Q}^{(e)} \cdot \hat{\mathbf{R}} \right)_{\parallel} - \right. \end{aligned}$$

$$\begin{aligned} & -\frac{k^2}{2}\hat{\mathbf{R}} \times \left(\mathbf{Q}^{(m)} \cdot \hat{\mathbf{R}} \right)_{\parallel} - \frac{ik^3}{3} \left(\mathbf{Q}^{(T)} \cdot \hat{\mathbf{R}} \right)_{\parallel} + \\ & + ik^3 \left(\left(\mathbf{O}^{(e)} \cdot \hat{\mathbf{R}} \right) \cdot \hat{\mathbf{R}} \right)_{\parallel} - \\ & \left. -\frac{ik^3}{180}\hat{\mathbf{R}} \times \left(\left(\mathbf{O}^{(m)} \cdot \hat{\mathbf{R}} \right) \cdot \hat{\mathbf{R}} \right)_{\parallel} \right] \cdot \exp(-ikR) \quad (9) \end{aligned}$$

Equation (9) describes electric field emitted by an infinitely large two-dimensional array of meta-molecules (or any sub-wavelength emitters) with induced oscillations of charge-current density approximated by first 8 dynamic multipoles. It contains 10 terms corresponding to the electric (\mathbf{p}), toroidal (\mathbf{T}) and magnetic (\mathbf{m}) dipoles, electric ($\mathbf{Q}^{(e)}$), magnetic ($\mathbf{Q}^{(m)}$) and toroidal ($\mathbf{Q}^{(T)}$) quadrupoles, electric ($\mathbf{O}^{(e)}$) and magnetic ($\mathbf{O}^{(m)}$) octupoles, and the so-called mean square radii of toroidal ($\mathbf{T}^{(1)}$) and magnetic ($\mathbf{m}^{(1)}$) dipoles, which are the lowest-order corrections retained to account for the finite size of the meta-molecules³⁶. Further multipole contributions to the radiation by an array can be found in the same way.

Using Eq. (9), the radiation transmitted and reflected by the two-dimensional array, when it is subjected to illumination by normally incident plane wave, can be found from:

$$\begin{aligned} \mathbf{E}_{reflected} &= [\mathbf{E}_s]_{\hat{\mathbf{R}}=-\hat{\mathbf{k}}} \\ \mathbf{E}_{transmitted} &= [\mathbf{E}_s]_{\hat{\mathbf{R}}=\hat{\mathbf{k}}} + \mathbf{E}_{incident} \end{aligned}$$

where $\hat{\mathbf{k}} = \mathbf{k}/k$ points in the direction of propagation of the incident radiation.

Below we will illustrate application of our approach for calculation of electromagnetic response of a metamaterial designed to exhibit strong toroidal resonance in the mid-IR part of the spectrum. The unit cell of the metamaterial array, shown in Fig. 3, contains a three-dimensional complex-shaped gold meta-molecule with the main features of the four-split-ring design proposed by Kaelberer *et al.*¹⁰. The current design was optimized for the novel metamaterial fabrication technique SAMPL³⁹, resulting in each of the four split rings being replaced with a pair of split rings of highly asymmetric shape, to reduce the effect of losses and maximize the contribution of the toroidal dipole moment. The transmission and reflection of the array of such meta-molecules were simulated in 14.5 μm – 23.5 μm wavelength range (see Appendix for material constants) using full 3D Maxwell's equations solver (COMSOL Multiphysics 3.5a). The numerical model also provided data on spatial distribution of the current densities, which were used to calculate dynamic multipole moments induced in each meta-molecule (see Appendix).

The simulated transmission and reflection spectra are shown in Fig. 4a,b as solid curves, revealing two distinct resonances located at around 21.0 μm and 17.4 μm . The numerical spectra are very well matched by the results

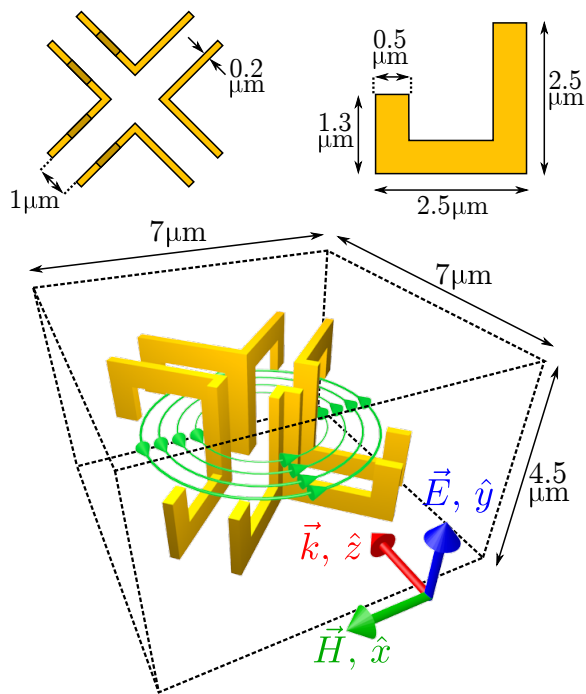


Figure 3: **The unit cell of the test case toroidal metamaterial.** The metamaterial is created by translating the unit cell along the \hat{x} and \hat{y} directions. The unit cell consists of four pairs of gold split-ring resonators that are embedded in the SU-8 polymer. The metamaterial is driven by the radiation propagating along the \hat{z} -axis and polarized along \hat{y} -axis. The configuration of the magnetic field that gives rise to the toroidal dipole response in the metamaterial is schematically illustrated with green field-lines.

of the multipole calculations described above (see dashed curves in Fig. 4a). Small discrepancies are attributed to somewhat limited accuracy of extracting the induced current distribution from the numerical model. The shorter-wavelength resonance corresponds to strong toroidal response, which is confirmed by our analysis of the multipole scattering presented in Fig. 4c (only four leading multipoles are shown). It shows that, for each meta-molecule, the power scattered by the induced toroidal dipole at $17.4 \mu\text{m}$ is more than three times larger than the contribution from any standard multipole, and therefore toroidal dipole excitation must play the key role in forming the metamaterial macroscopic response at this wavelength. This can be verified directly by excluding the toroidal dipole moment from the multipole-based calculations of the transmission and reflection. As one can see from Fig. 4b the correct replication of the resonant features is simply not possible in the frame of the standard multipole expansion, and the notion of the toroidal dipole is thus crucial for the correct interpretation of the macroscopic response of metamaterial.

In conclusion, we developed a fully analytical formalism that allows calculating the transmission and reflection properties of thin sheets of metamaterials and ma-

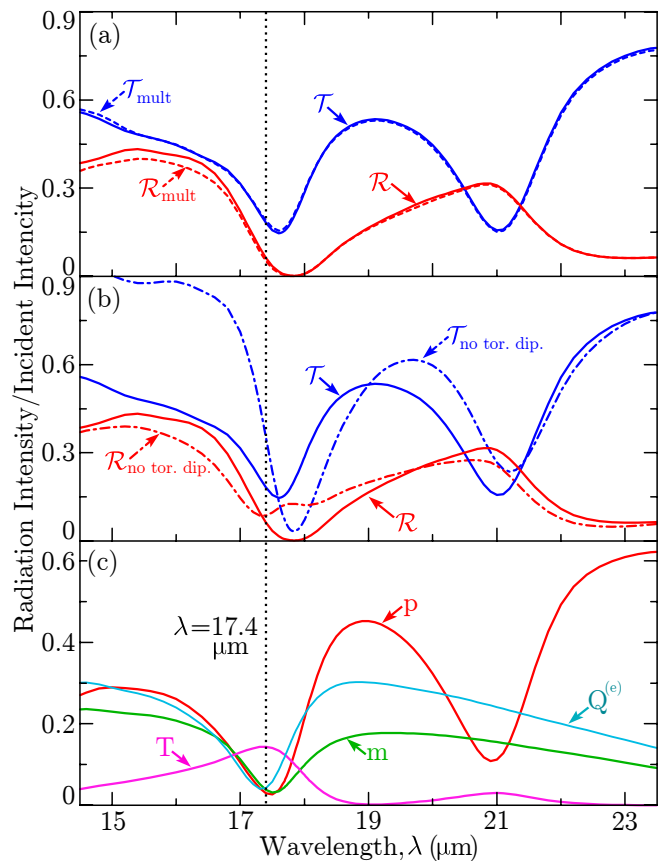


Figure 4: **Macroscopic response of the test case toroidal metamaterial.** The response of the metamaterial on Fig. 3 has been modeled using the realistic material constants for gold and SU-8 polymer (see Appendix). (a) Transmission (\mathcal{T} ; blue) and reflection (\mathcal{R} ; red) of the metamaterial. The solid curves (\mathcal{T} , \mathcal{R}) are obtained directly from numerical solution of Maxwell's equations, dashed curves ($\mathcal{T}_{\text{mult}}$, $\mathcal{R}_{\text{mult}}$) are obtained using Eq. (9), from the multipole moment representation of each meta-molecule of the metamaterial. (b) The comparison of the directly calculated metamaterial transmission and reflection (\mathcal{T} , \mathcal{R} ; solid curves) to the response obtained from multipoles but without the input of toroidal dipole ($\mathcal{T}_{\text{no tor. dip.}}$, $\mathcal{R}_{\text{no tor. dip.}}$; dash-dot curves). (c) Intensity of the radiation scattered back (i.e. reflected) by each of four leading multipoles when placed in an array (\mathbf{p} -electric dipole, \mathbf{m} -magnetic dipole, \mathbf{T} -toroidal dipole, $\mathbf{Q}^{(e)}$ -electric quadrupole). The radiation intensity in all three plots is normalized with respect to incident radiation (that induces the multipoles).

terial composites, based on the dynamic multipole decomposition of charge-current densities induced in their structure by an incident electromagnetic wave. Further to the derived formalism, we provided a case study which proved that the contribution of the toroidal dipole is crucial for the correct interpretation of the reflection and the transmission spectra of a certain class of metamaterials. Our findings demonstrate that the toroidal dipole may be dominant in the response of the electromagnetic media, and therefore cannot be treated simply as a high-order

correction to the electric or magnetic multipoles.

Acknowledgments

The authors acknowledge the support of the Engineering and Physical Sciences Research Council U.K., the Royal Society and of the MOE Singapore grant MOE2011-T3-1-005. The authors would also like to thank Dr. I. Brener and Dr. D. B. Burckel from Sandia National Laboratories (US) for providing the material data and discussions.

Appendix

Integral involving the Spherical Harmonics - $I_{l,m}$

Here we will derive the Eq. (7). At the core of the derivation lies the evaluation of the following integral:

$$\int_R^\infty dr \left(\frac{R}{r}\right)^q \exp(-ikr) \cong \frac{\exp(-ikR)}{ik}, \quad \Im(k) < 0 \quad (10)$$

The case $q = 0$ can be found by the direct integration. Higher order cases can be evaluated by relating them to the exponential integrals. Abramowitz and Stegun⁴⁰ define the exponential integral as (Eq. (5.1.4) of Ref. [40]):

$$E_n(z) = \int_1^\infty dt \frac{\exp(-zt)}{t^n}, \quad n = 0, 1, 2, \dots \quad \Re(z) > 0$$

We are interested in the asymptotic expansion of the $E_n(z)$ for the case of large z given in Eq. (5.1.51) of Ref. [40]:

$$\lim_{z \rightarrow \infty} E_n(z) \cong \frac{\exp(-z)}{z} (1 - O(1/z)), \quad |\arg(z)| < \frac{3}{2}\pi$$

Equation (10) can therefore as be evaluated as follows:

$$\begin{aligned} \int_R^\infty dr \left(\frac{R}{r}\right)^q \exp(-ikr) &= R \cdot E_q(ikR) \cong \\ &\cong R \cdot \frac{\exp(-ikR)}{ikR} \cdot (1 - O(1/kR)) \end{aligned}$$

Note that $\Im(k) < 0$ implies $\Re(ikR) > 0$ and $|\arg(ikR)| < \pi/2$. Up to order $O(1/kR)$ or, equivalently, up to $O(\lambda/R)$, the expression becomes:

$$\int_R^\infty dr \left(\frac{R}{r}\right)^q \exp(-ikr) \cong \frac{\exp(-ikR)}{ik}$$

We now turn our attention to Eq. (6):

$$I_{l,m} = \int d^2r Y_{l,m}(\theta, \phi) \exp(-ikr) / r$$

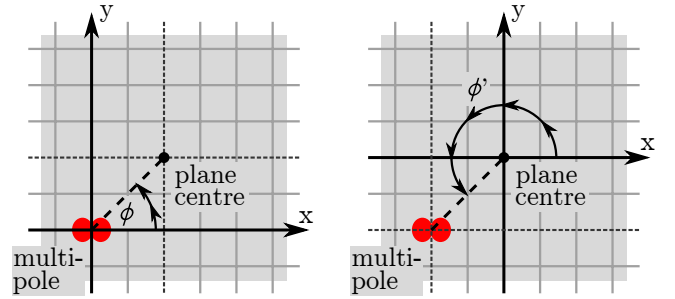


Figure 5: **The difference between ϕ and ϕ' .** Angle ϕ is defined in the coordinate frame of a multipole under consideration, whilst the angle ϕ' is defined in the coordinate frame of the multipole array (also see Fig. 2). The observer (see Fig. 2) is located directly above the origin of the array.

The integration is understood to be over the area of the array of multipoles as shown in Fig. 2. The position of each multipole in the plane of the array is given by ρ , the distance between the centre-point of the array and the considered multipole, and ϕ' the angle between the x-axis and the vector connecting the centre-point of the array and the multipole in question. There is also another angle ϕ that belongs together with r and θ , and denotes the position of the observer relative to the multipole under consideration (see Fig. 2). It is convenient to place the origin of the multipole array directly below the observer. In this case the relation between ϕ and ϕ' takes a simple form $\phi = \phi' + \pi$, up to a full rotation around 2π . Figure 5 helps to visualize the two angles. The same choice of origin establishes the relation $r^2 = \rho^2 + R^2$.

One can now rewrite the integral in more accessible way:

$$I_{l,m} = \int_0^{2\pi} d\phi' \int_0^\infty \rho d\rho Y_{l,m}(\theta, \phi' + \pi) \frac{\exp(-ikr)}{r}$$

From $r^2 = \rho^2 + R^2$ it follows that $r dr = \rho d\rho$, so

$$\begin{aligned} I_{l,m} &= \int_0^{2\pi} d\phi' \int_R^\infty r dr Y_{l,m}(\theta, \phi' + \pi) \frac{\exp(-ikr)}{r} \\ &= (-1)^{m+m} \sqrt{\frac{2l+1}{4\pi} \frac{(l-m)!}{(l+m)!}} \\ &\quad \cdot \int d\phi' \exp(im\phi') \int_R^\infty dr P_l^m(\cos\theta) \exp(-ikr) \end{aligned}$$

In the last step, we have expanded the spherical harmonic following the convention used by Arfken and Weber (see Chapter 12.6 in Ref. [41]), and substituted $\exp(im(\pi + \phi')) = (-1)^m \exp(im\phi')$. Here the P_l^m denotes the Associated Legendre Functions. The expression above is simplified considerably by the fact that the integral over ϕ' is non-zero only for $m = 0$:

$$I_{l,m} = \pi \delta_{m,0} \sqrt{\frac{2l+1}{\pi}} \int_R^\infty dr P_l(\cos\theta) \exp(-ikr)$$

Above we have used $P_l^0(x) = P_l(x)$ to replace the Associated Legendre Functions with Legendre Polynomials (respectively). From Fig. 2 it follows that $\cos\theta = R/r$ for $\mathbf{R} = R\hat{\mathbf{z}}$, and $\cos\theta = -R/r$ for $\mathbf{R} = -R\hat{\mathbf{z}}$, thus $\cos\theta = (\hat{\mathbf{R}} \cdot \hat{\mathbf{z}}) \times R/r$. Using the parity property of Legendre Polynomials (Eq. (12.37) in Ref. [41]) one obtains $P_l(\cos\theta) = (\hat{\mathbf{R}} \cdot \hat{\mathbf{z}})^l P_l(R/r)$. Being a polynomial $P_l(x)$ can be expressed as power series $P_l(x) = \sum_{s=0}^{\infty} a_s^{(l)} x^s$, the integral then becomes (with use of Eq. (10)):

$$\begin{aligned} I_{l,m} &= \pi \delta_{m,0} \sqrt{\frac{2l+1}{\pi}} (\hat{\mathbf{R}} \cdot \hat{\mathbf{z}})^l \cdot \\ &\quad \cdot \sum_{s=0}^{\infty} a_s^{(l)} \int_R^{\infty} dr \left(\frac{R}{r}\right)^s \exp(-ikr) \approx \\ &\approx \pi \delta_{m,0} \sqrt{\frac{2l+1}{\pi}} (\hat{\mathbf{R}} \cdot \hat{\mathbf{z}})^l \sum_{s=0}^{\infty} a_s^{(l)} \cdot \\ &\quad \cdot \left(\frac{\exp(-ikR)}{ik} + O(\lambda/R) \right) \end{aligned}$$

Finally, one uses the normalization of the Legendre Polynomials to eliminate the sum $P_l(1) = 1 = \sum_{s=0}^{\infty} a_s^{(l)}$ (Eq. (12.31) in Ref. [41]). Thus

$$I_{l,m} \approx \frac{\pi \delta_{m,0} (\hat{\mathbf{R}} \cdot \hat{\mathbf{z}})^l}{ik} \cdot \sqrt{\frac{2l+1}{\pi}} \cdot \exp(-ikR)$$

which completes the derivation.

Multipole decomposition of the radiation from a localized source

To derive the formula for the electric field radiated by the array of multipoles (see Eq. (9)) we have used the expression for the radiation emitted by the single multipole sources provided by Radescu and Vaman (see Eq. (3.15) in Ref. [36]). Here we will give the truncated series for the electric field emitted by the multipole sources, in the SI units, and for the complex-valued harmonic time-dependence of the source ($\sim \exp(+i\omega t)$).

Due to large number of terms it is convenient to separate the series into different orders of l . The $l = 1$ sub-series then contain the dipolar contributions:

$$\begin{aligned} \mathbf{E}_{(l=1)} &\approx \frac{\mu_0 c^2}{3\sqrt{2\pi}} \cdot \frac{\exp(-ikr)}{r} \cdot \sum_{m=0,\pm 1} \left[\right. \\ &\quad \left. \left(k^2 Q_{1,m} - ik^3 T_{1,m} + ik^5 T_{1,m}^{(1)} \right) \cdot \right. \\ &\quad \cdot \left(\mathbf{Y}_{1,2,m} + \sqrt{2} \mathbf{Y}_{1,0,m} \right) + \\ &\quad \left. + i\sqrt{3} \left(k^2 M_{1,m} - k^4 M_{1,m}^{(1)} \right) \cdot \mathbf{Y}_{1,1,m} \right] \end{aligned}$$

$l = 2$ sub-series contain the quadrupolar contributions:

$$\begin{aligned} \mathbf{E}_{(l=2)} &\approx \frac{\mu_0 c^2}{10\sqrt{6\pi}} \cdot \frac{\exp(-ikr)}{r} \cdot \sum_{m=0,\pm 1,\pm 2} \left[\right. \\ &\quad \left. \left(ik^3 Q_{2,m}^{(e)} + k^4 Q_{2,m}^{(T)} \right) \cdot \right. \\ &\quad \left. \left(\sqrt{2} \mathbf{Y}_{2,3,m} + \sqrt{3} \mathbf{Y}_{2,1,m} \right) - \right. \\ &\quad \left. - \sqrt{5} k^3 Q_{2,m}^{(m)} \mathbf{Y}_{2,2,m} \right] \end{aligned}$$

$l = 3$ sub-series contain the octupolar contributions:

$$\begin{aligned} \mathbf{E}_{(l=3)} &\approx - \frac{\mu_0 c^2 k^4}{15\sqrt{3\pi}} \cdot \frac{\exp(-ikr)}{r} \cdot \sum_{m=0,\pm 1,\pm 2,\pm 3} \left[\right. \\ &\quad \left. \frac{1}{7} O_{3,m}^{(e)} \cdot \left(\sqrt{3} \mathbf{Y}_{3,4,m} + 2 \mathbf{Y}_{3,2,m} \right) + \right. \\ &\quad \left. + \frac{i}{\sqrt{7}} O_{3,m}^{(m)} \mathbf{Y}_{3,3,m} \right] \end{aligned}$$

The total field emitted is given by:

$$\mathbf{E} = \mathbf{E}_{(l=1)} + \mathbf{E}_{(l=2)} + \mathbf{E}_{(l=3)} + (l > 3 \text{ sub-series})$$

The series given above are truncated at order k^4 , but the first-order correction for the toroidal dipole ($T_{1,m}^{(1)}$), of order k^5 , is also included to avoid errors in the spectral range where toroidal dipole dominates (see Fig. 4). The other k^5 terms that can be included are the toroidal octupole, the electric and magnetic hexadecapoles ($l = 4$), and the first-order correction to the magnetic quadrupole.

One may notice, that no correction terms for the electric dipoles have been included. Radescu and Vaman³⁶ have shown that the correction terms for the electric multipoles do not contribute to the far-field radiation emitted by arbitrary localized charge-current density distributions. The correction terms for the magnetic and toroidal multipoles, by contrast, do contribute.

Integrals for finding the leading multipoles from a current distribution

The expressions we have used to calculate the multipole moments from the current density distribution are those given by Radescu and Vaman³⁶. We will repeat them here for convenience. Note that the electric and magnetic multipoles are exactly the same as the ones given in the standard texts on electrodynamics¹⁷ (apart from the different normalization constants).

Cartesian multipoles are computed by integrating over the charge density ($\rho(\mathbf{r})$) or current density ($\mathbf{J}(\mathbf{r})$) distribution within the unit cell ($\alpha, \beta, \gamma = x, y, z$):

$$p_\alpha = \int d^3r \rho r_\alpha = \frac{1}{i\omega} \int d^3r J_\alpha$$

$$\begin{aligned}
m_\alpha &= \frac{1}{2c} \int d^3r [\mathbf{r} \times \mathbf{J}]_\alpha \\
m_\alpha^{(1)} &= \frac{1}{2c} \int d^3r [\mathbf{r} \times \mathbf{J}]_\alpha r^2 \\
T_\alpha &= \frac{1}{10c} \int d^3r [(\mathbf{r} \cdot \mathbf{J}) r_\alpha - 2r^2 J_\alpha] \\
T_\alpha^{(1)} &= \frac{1}{28c} \int d^3r [3r^2 J_\alpha - 2r_\alpha (\mathbf{r} \cdot \mathbf{J})] r^2 \\
Q_{\alpha,\beta}^{(e)} &= \frac{1}{2} \int d^3r \rho \left[r_\alpha r_\beta - \frac{1}{3} \delta_{\alpha,\beta} r^2 \right] = \\
&= \frac{1}{i2\omega} \int d^3r \left[r_\alpha J_\beta + r_\beta J_\alpha - \frac{2}{3} \delta_{\alpha,\beta} (\mathbf{r} \cdot \mathbf{J}) \right] \\
Q_{\alpha,\beta}^{(m)} &= \frac{1}{3c} \int d^3r [\mathbf{r} \times \mathbf{J}]_\alpha r_\beta + \{\alpha \leftrightarrow \beta\} \\
Q_{\alpha,\beta}^{(T)} &= \frac{1}{28c} \int d^3r \left[4r_\alpha r_\beta (\mathbf{r} \cdot \mathbf{J}) - 5r^2 (r_\alpha J_\beta + r_\beta J_\alpha) + \right. \\
&\quad \left. + 2r^2 (\mathbf{r} \cdot \mathbf{J}) \delta_{\alpha,\beta} \right] \\
O_{\alpha,\beta,\gamma}^{(e)} &= \frac{1}{6} \int d^3r \rho r_\alpha \left(r_\beta r_\gamma - \frac{1}{5} r^2 \delta_{\beta,\gamma} \right) + \\
&\quad + \{\alpha \leftrightarrow \beta, \gamma\} + \{\alpha \leftrightarrow \gamma, \beta\} \\
&= \frac{1}{i6\omega} \int d^3r \left[J_\alpha \left(r_\beta r_\gamma - \frac{r^2}{5} \delta_{\beta,\gamma} \right) + \right. \\
&\quad \left. + r_\alpha \left(J_\beta r_\gamma + r_\beta J_\gamma - \frac{2}{5} (\mathbf{r} \cdot \mathbf{J}) \delta_{\beta,\gamma} \right) \right] + \\
&\quad + \{\alpha \leftrightarrow \beta, \gamma\} + \{\alpha \leftrightarrow \gamma, \beta\} \\
O_{\alpha,\beta,\gamma}^{(m)} &= \frac{15}{2c} \int d^3r \left(r_\alpha r_\beta - \frac{r^2}{5} \delta_{\alpha,\beta} \right) \cdot [\mathbf{r} \times \mathbf{J}]_\gamma + \\
&\quad + \{\alpha \leftrightarrow \beta, \gamma\} + \{\alpha \leftrightarrow \gamma, \beta\}
\end{aligned}$$

For quadrupoles and octupoles a short-hand has been used to improve clarity. For example: $\int d^3r [\mathbf{r} \times \mathbf{J}]_\alpha r_\beta + \{\alpha \leftrightarrow \beta\} \equiv \int d^3r [\mathbf{r} \times \mathbf{J}]_\alpha r_\beta + \int d^3r [\mathbf{r} \times \mathbf{J}]_\beta r_\alpha$, i.e. the second term is obtained from the first term, with the exchanged positions of indices α and β . In case of octupoles (for example):

$$\frac{1}{6} \int d^3r \rho r_\alpha \left(r_\beta r_\gamma - \frac{1}{5} r^2 \delta_{\beta,\gamma} \right) + \{\alpha \leftrightarrow \beta, \gamma\} + \{\alpha \leftrightarrow \gamma, \beta\}$$

means that the second term is obtained from the first term by exchanging α and β whilst leaving γ untouched. The third term is, again, obtained from the first term, but this time α and γ are exchanged, whilst β remains untouched.

In the time-harmonic case there is no clear difference between the conduction and displacement currents. In simulations we have used $\mathbf{J} = i\omega\epsilon_0 (\tilde{\epsilon}_r - 1) \mathbf{E}$ to find the current density within the media, from the electric field distribution $\mathbf{E}(\mathbf{r})$. The relevant quantities are: ω -angular frequency, ϵ_0 -free-space permittivity, c -speed of light, and $\tilde{\epsilon}_r$ -complex-valued dielectric constant (used to describe both the dielectrics and metals).

The spherical multipoles are related to the Cartesian

multipoles through:

$$\begin{aligned}
Q_{1,0} &= p_z, & Q_{1,\pm 1} &= (\mp p_x + i p_y) / \sqrt{2} \\
M_{1,0} &= -m_z, & M_{1,\pm 1} &= (\pm m_x - i m_y) / \sqrt{2} \\
M_{1,0}^{(1)} &= -m_z^{(1)}, & M_{1,\pm 1}^{(1)} &= (\pm m_x^{(1)} - i m_y^{(1)}) / \sqrt{2} \\
T_{1,0} &= T_z, & T_{1,\pm 1} &= (\mp T_x + i T_y) / \sqrt{2} \\
T_{1,0}^{(1)} &= -T_z^{(1)}, & T_{1,\pm 1}^{(1)} &= (\pm T_x^{(1)} - i T_y^{(1)}) / \sqrt{2} \\
Q_{2,0}^{(e)} &= 3Q_{zz}^{(e)}, & Q_{2,\pm 1}^{(e)} &= \sqrt{6} (\mp Q_{xz}^{(e)} + i Q_{yz}^{(e)}) \\
Q_{2,\pm 2}^{(e)} &= \frac{\sqrt{6}}{2} (Q_{xx}^{(e)} \mp i 2Q_{xy}^{(e)} - Q_{yy}^{(e)}) \\
Q_{2,0}^{(m)} &= -\frac{3}{2} Q_{zz}^{(m)}, & Q_{2,\pm 1}^{(m)} &= \sqrt{\frac{3}{2}} (\pm Q_{xz}^{(m)} - i Q_{yz}^{(m)}) \\
Q_{2,\pm 2}^{(m)} &= \frac{\sqrt{6}}{4} (-Q_{xx}^{(m)} \pm i 2Q_{xy}^{(m)} + Q_{yy}^{(m)}) \\
Q_{2,0}^{(T)} &= Q_{zz}^{(T)}, & Q_{2,\pm 1}^{(T)} &= \sqrt{\frac{2}{3}} (\mp Q_{xz}^{(T)} + i Q_{yz}^{(T)}) \\
Q_{2,\pm 2}^{(T)} &= (Q_{xx}^{(T)} \mp i 2Q_{xy}^{(T)} - Q_{yy}^{(T)}) / \sqrt{6} \\
O_{3,0}^{(e)} &= 15O_{zzz}^{(e)} \\
O_{3,\pm 1}^{(e)} &= \mp \frac{15\sqrt{3}}{2} (O_{zzz}^{(e)} \pm i O_{yyy}^{(e)} \pm i O_{xxy}^{(e)}) \\
O_{3,\pm 2}^{(e)} &= -3\sqrt{\frac{15}{2}} (O_{zzz}^{(e)} + 2O_{yyz}^{(e)} \pm i 2O_{xyz}^{(e)}) \\
O_{3,\pm 3}^{(e)} &= \mp \frac{3\sqrt{5}}{2} (O_{xxx}^{(e)} - 3O_{yyx}^{(e)} \pm i O_{yyy}^{(e)} \mp i 3O_{xxy}^{(e)}) \\
O_{3,0}^{(m)} &= -O_{zzz}^{(m)} / 12 \\
O_{3,\pm 1}^{(m)} &= \pm (O_{zzz}^{(m)} \pm i O_{yyy}^{(m)} \pm i O_{xxy}^{(m)}) / 8\sqrt{3} \\
O_{3,\pm 2}^{(m)} &= \frac{\sqrt{2}}{8\sqrt{15}} (O_{zzz}^{(m)} + 2O_{yyz}^{(m)} \pm i 2O_{xyz}^{(m)}) \\
O_{3,\pm 3}^{(m)} &= \pm (O_{xxx}^{(m)} - 3O_{yyx}^{(m)} \pm i O_{yyy}^{(m)} \mp i 3O_{xxy}^{(m)}) / 24\sqrt{5}
\end{aligned}$$

Material constants used in simulations

The constants of the materials used for simulations have been measured and provided by Sandia National Laboratories (US) in a private communication. An infrared variable angle spectroscopic ellipsometer (J. A. Woolam) was used to measure Ψ and Δ , from which the optical constants were derived. The same constants have been used to model the response of the previously demonstrated 3D cubic metamaterial based on SAMPL technology³⁹.

The refractive index of the SU8 polymer that housed the gold split ring resonators ($\tilde{n} = n + ik$; negative k implies losses) is shown in Fig. 6. The dielectric constant of the gold used for simulations is shown in Fig. 7 ($\tilde{\epsilon}_r = \epsilon'_r + i\epsilon''_r$; negative ϵ''_r implies losses).

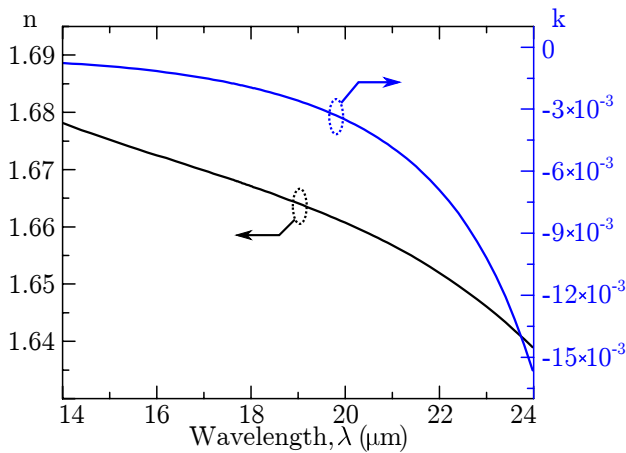


Figure 6: **The refractive index of the polymer SU8 used for simulating the case-study metamaterial.** The complex-valued refractive index of SU8 is given by $\tilde{n} = n + ik$.

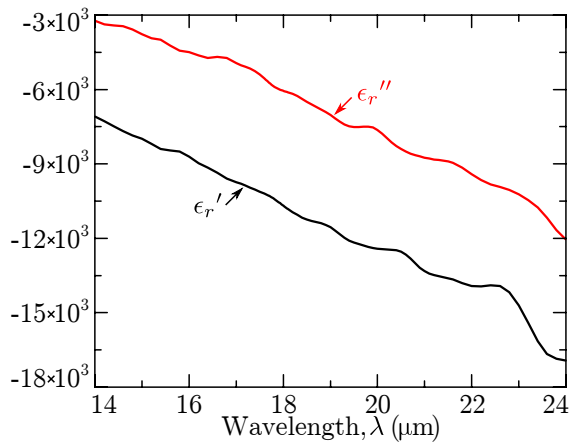


Figure 7: **The dielectric constant of the gold used for simulating the case-study metamaterial.** The complex-valued dielectric constant is given by $\tilde{\epsilon}_r = \epsilon_r' + i\epsilon_r''$

References

* Electronic address: vs1106@orc.soton.ac.uk

1. Zel'dovich, Ya. B., "Electromagnetic interaction with parity violation," *Sov. Phys. JETP*, vol. 33, pp. 1184–1186, 1957.
2. Wood, C. S. *et al.*, "Measurement of parity nonconservation and an anapole moment in cesium," *Science*, vol. 275, pp. 1759–1763, 1997.
3. Papasimakis, N., Fedotov, V. A., Marinov, K. & Zheludev, N. I., "Gyrotropy of a metamolecule: wire on a torus," *Phys. Rev. Lett.*, vol. 103, p. 093901, 2009.
4. Marinov, K., Boardman, A. D., Fedotov, V. A. & Zheludev, N., "Toroidal metamaterial," *New J. Phys.*, vol. 9, p. 324, 2007.
5. Afanasiev, G. N., "Simplest sources of electromagnetic fields as a tool for testing the reciprocity-like theorems," *J. Phys. D: Appl. Phys.*, vol. 34, pp. 539–559, 2001.
6. Afanasiev, G. N. & Stepanovsky, Yu. P., "The electromagnetic field of elementary time-dependent toroidal sources," *J. Appl. Phys. A*, vol. 28, pp. 4565–4580, 1995.
7. Marengo, E. A. & Ziolkowski, R. W., "Nonradiating sources, the Aharonov-Bohm effect, and the question of measurability of electromagnetic potentials," *Radio Sci.*, vol. 37, p. 19, 2002.
8. Broadman, A. D., Marinov, K., Zheludev, N. I. & Fedotov, V. A., "Dispersion properties of nonradiating configurations: Finite-difference time-domain modelling," *Phys. Rev. E*, vol. 72, p. 036603, 2005.
9. Fedotov, V. A., Rogacheva, A. V., Savinov, V., Tsai, D. P. & Zheludev, N. I., "Non-trivial non-radiating excitation as a mechanism of resonant transparency in toroidal metamaterials," *arXiv:1211.3840v1*, 2012.
10. Kaelberer, T., Fedotov, V. A., Papasimakis, N., Tsai, D. P. & Zheludev, N. I., "Toroidal dipole response in a metamaterial," *Science*, vol. 330, pp. 1510–1512, 2010.
11. Dong, Z.-G., Ni, P., Zhu, J. & Zhang, X., "Toroidal dipole response in a multifold double-ring metamaterial," *Opt. Express*, vol. 20, pp. 13 065–13 070, 2012.
12. Dong, Z.-G., Zhu, J., Rho, J., Li, J.-Q., Lu, C., Yin, X. & Zhang, X., "Optical toroidal dipolar response by an asymmetric double-bar metamaterial," *Appl. Phys. Lett.*, vol. 101, p. 144105, 2012.
13. Qgüt, B., Talebi, N., Vogelgesang, R., Sigle, W. & van Aken, P. A., "Toroidal plasmonic eigenmodes in oligomer nanocavities for the visible," *Nano Lett.*, vol. 12, pp. 5239–5244, 2012.
14. Fan, Y., Wei, Z., Li, H., Chen, H. & Soukoulis, C. M., "Low-loss and high-Q planar metamaterial with toroidal moment," *Phys. Rev. B*, vol. 87, p. 115417, 2013.
15. Huang, Y.-W. *et al.*, "Design of plasmonic toroidal metamaterials at optical frequencies," *Opt. Express*, vol. 20, pp. 1760–1768, 2012.
16. Huang, Y.-W., Chen, W. T., Wu, P. C., Fedotov, V. A., Zheludev, N. I. & Tsai, D. P., "Toroidal lasing spaser," *Sci. Rep.*, vol. 3, p. 1237, 2013.
17. Jackson, J. D., *Classical Electrodynamics*, 3rd ed. New York: Wiley, 1999.
18. Zheludev, N. I., "The road ahead for metamaterials," *Science*, vol. 328, pp. 582–583, 2010.
19. Soukoulis, C. M. & Wegener, M., "Past achievements and future challenges in the development of three-dimensional photonic metamaterials," *Nature Photon.*, vol. 5, pp. 523–530, 2011.
20. Liu, Y. & Zhang, X., "Metamaterials: a new frontier of science and technology," *Chem. Soc. Rev.*, vol. 40, pp. 2494–2507, 2011.
21. Simovski, C. R., "On electromagnetic characterization and homogenization of nanostructured metamaterials," *J. Opt.*, vol. 13, p. 013001, 2011.
22. Chipouline, A., Simovski, C. & Tretyakov, S., "Basics of averaging of the Maxwell equations for bulk materials," *Metamaterials*, vol. 6, pp. 77–120, 2012.
23. Engheta, N., Murphy, W. D., Rokhlin, V. & Vassiliou, M. S., "The fast multipole method (FMM) for electromagnetic scattering problems," *IEEE Trans. Antennas Propag.*, vol. 40, pp. 634–641, 1992.
24. Coifman, R., Rokhlin, V. & Wandzura, S., "The fast multipole method for the wave equation: a pedestrian prescription," *IEEE Antennas Propag. Mag.*, vol. 35, pp. 7–12, 1993.
25. Lu, C. C. & Chew, W. C., "Fast algorithm for solving hybrid integral equations," *IEE Proc. H, Microw. Antennas Propag.*, vol. 140, pp. 455–460, 1993.

26. Craeye, C., "A fast Impedance and pattern computation scheme for finite antenna arrays," *IEEE Trans. Antennas Propag.*, vol. 54, pp. 3030–3034, 2006.
27. Lu, W. B. & Cui, T. J., "Efficient method for full-wave analysis of large-scale finite-sized periodic structures," *J. of Electromagn. Waves and Appl.*, vol. 21, pp. 2157–2168, 2007.
28. Shubair, R. M. & Chow, Y. L., "Efficient computation of the periodic Green's function in layered dielectric media," *IEEE Trans. Microw. Theory Techn.*, vol. 41, pp. 498–502, 1993.
29. Fructos, A. L., Boix, R. R., Mesa, F. & Medina, F., "An efficient approach for the computation of 2-D Green's functions with 1-D and 2-D periodicities in homogeneous media," *IEEE Trans. Antennas Propag.*, vol. 56, pp. 3733–3742, 2008.
30. Valerio, G., Baccarelli, P., Burghignoli, P. & Galli, A., "Comparative analysis of acceleration techniques for 2-D and 3-D Green's functions in periodic structures along one and two directions," *IEEE Trans. Antennas Propag.*, vol. 55, pp. 1630–1643, 2007.
31. Saadoun, M. M. I. & Engheta, N., "Theoretical study of electromagnetic properties of non-local Ω media," *PIER*, vol. 9, pp. 351–397, 1994.
32. Bahr, A. J. & Clausig, K. R., "An approximate model for artificial chiral material," *IEEE Trans. Antennas Propag.*, vol. 42, pp. 1592–1599, 1994.
33. Pendry, J. B., Holden, A. J., Robbins, D. J. & Stewart, W. J., "Magnetism from conductors and enhanced non-linear phenomena," *IEEE Trans. Microw. Theory Techn.*, vol. 47, pp. 2075–2084, 1999.
34. Rockstuhl, C. *et al.*, "The origin of magnetic polarizability in metamaterials at optical frequencies - an electrodynamic approach," *Opt. Express*, vol. 15, pp. 8871–8883, 2007.
35. Sten, J. C.-E. & Sjöberg, D., "Low-frequency scattering analysis and homogenization of split-ring elements," *PIER B*, vol. 35, pp. 187–212, 2011.
36. Radescu, E. E. & Vaman, G., "Exact calculation of the angular momentum loss, recoil force, and radiation intensity for an arbitrary source in terms of electric, magnetic, and toroid multipoles," *Phys. Rev. E*, vol. 65, p. 046609, 2002.
37. Akhiezer, A. I. & Berestetskii, V. B., *Quantum Electrodynamics*, 2nd ed. New York: Interscience Publishers, 1965.
38. Dubovik, V. M. & Cheshkov, A. A., "Multipole expansion in classical and quantum field theory and radiation," *Sov. J. Part. Nucl.*, vol. 5, pp. 318–337, 1975.
39. Bruckel, D. B. *et al.*, "Micrometer-scale cubic unit cell 3D metamaterial layers," *Adv. Mater.*, vol. 22, pp. 5053–5057, 2010.
40. Abramowitz, M. & Stegun, I. A., *Handbook of Mathematical Functions with Formulas, Graphs, and Mathematical Tables*, 10th ed. Dover Publications, 1972.
41. Arfken, G. B. & Weber, H. J., *Mathematical Methods for Physicists*, 5th ed. Harcourt/Academic Press, 2001.